Franz Selzer, Nelli Weiß, David Kneppe, Ludwig Bormann, Christoph Sachse, Nikolai Gaponik, Alexander Eychmüller, Karl Leo, Lars Müller-Meskamp

A spray-coating process for highly conductive silver nanowire networks as the transparent top-electrode for small molecule organic photovoltaics

Erstveröffentlichung in / First published in:
Nanoscale. 2015, 7(6), S. 2777–2783 [Zugriff am: 04.11.2019]. Royal Society of Chemistry. ISSN 2040-3372.

DOI: https://doi.org/10.1039/c4nr06502f

Nanoscale

PAPER

View Article Online
View Journal | View Issue

Cite this: *Nanoscale*, 2015, **7**, 2777

A spray-coating process for highly conductive silver nanowire networks as the transparent top-electrode for small molecule organic photovoltaics†

Franz Selzer,*[a] Nelli Weiß,[b] David Kneppe,[a] Ludwig Bormann,[a] Christoph Sachse,[a] Nikolai Gaponik,[b] Alexander Eychmüller,[b] Karl Leo[a] and Lars Müller-Meskamp*[a]

We present a novel top-electrode spray-coating process for the solution-based deposition of silver nanowires (AgNWs) onto vacuum-processed small molecule organic electronic solar cells. The process is compatible with organic light emitting diodes (OLEDs) and organic light emitting thin film transistors (OLETs) as well. By modifying commonly synthesized AgNWs with a perfluorinated methacrylate, we are able to disperse these wires in a highly fluorinated solvent. This solvent does not dissolve most organic materials, enabling a top spray-coating process for sensitive small molecule and polymer-based devices. The optimized preparation of the novel AgNW dispersion and spray-coating at only 30 °C leads to high performance electrodes directly after the deposition, exhibiting a sheet resistance of 10.0 Ω $\square^{-1}$ at 87.4% transparency (80.0% with substrate). By spraying our novel AgNW dispersion in air onto the vacuum-processed organic p-i-n type solar cells, we obtain working solar cells with a power conversion efficiency (PCE) of 1.23%, compared to the air exposed reference devices employing thermally evaporated thin metal layers as the top-electrode.

Received 4th November 2014,
Accepted 23rd December 2014

DOI: 10.1039/c4nr06502f

www.rsc.org/nanoscale

Introduction

State-of-the-art silver nanowire (AgNW) networks are used as transparent bottom-electrodes for organic electronic devices (OEDs) based on small molecules or polymers.[1,2] A facile and scalable fabrication method for such electrodes is the spray-coating of nanowire dispersions.[3] The resulting networks exhibit a low sheet resistance (R_S) and high transmittance and allow the fabrication of flexible devices with equal performances compared to those comprising indium tin oxide (ITO).[4] However, common dispersing media like ethanol, other alcohols, or water are not compatible to the sensible OED stacks, limiting the nanowire technology to superstrate geometries only. Transferring the superior opto-electrical properties of nanowire bottom-electrodes to a transparent top-contact for OEDs would lead to a higher process flexibility and technological benefits. The expected light scattering from the nanowire network[5] could be used to enhance the power conversion efficiency (PCE) of an organic solar cell (OSC) due to an enlarged light path through the photoactive layer[6,7] or to enhance the efficiency and colour stability of organic light emitting diodes (OLEDs) over wider emission angles.[8,9] Since the wires are directly sprayed onto the organic stack, no planarization layers, as necessary for bottom-electrodes in small molecule devices,[1] are needed. These arguments and the option to use opaque substrates like metal foils render the application of AgNWs as transparent top-contact for OEDs very appealing.

The first successful approach was reported by Lee *et al.*, who laminated an AgNW network onto small molecule organic solar cells.[10] Recently, Krantz *et al.*,[11] Reinhard *et al.*[12] and Margulis *et al.*[13] published spray-coating of AgNWs onto polymer-based OSCs or solid-state dye-sensitized solar cells. In all the three articles, PEDOT:PSS was used as a protection layer to prevent the organic materials from being redissolved or damaged by the ethanol contained in the nanowire dispersion. Since lamination is not easily scalable and the use of PEDOT:PSS or other solution-based protection layers is not applicable to most small molecule stacks or is detrimental for device lifetimes, we have opted for an alternative scalable and non-harmful process. In addition, we strove to avoid acidic or water-based processes and materials that are not compatible with the desired stabilities and lifetimes.

[a]*Institute for Applied Photophysics, TU Dresden, George-Bähr-Straße 1, Dresden, D-01062, Germany. E-mail: franz.selzer@iapp.de*
[b]*Physical Chemistry, TU Dresden, Bergstraße 66b, Dresden, D-01062, Germany*
† Electronic supplementary information (ESI) available: XPS and SEM data clarifying the crucial role of the amount of stabilizer on sheet resistance; *j–V*-data of the annealed air cell enabling a deeper understanding of the influence of air exposure. See DOI: 10.1039/c4nr06502f.

Here, we present a method of producing a coating dispersion of AgNWs in an inert fluorinated solvent, which can be used for low temperature coating of transparent top-electrodes without dissolving or damaging the underlying organic layers. When deposited at only 30 °C substrate temperature, the spray-coated electrode exhibits a sheet resistance of 10.0 Ω $\square^{-1}$ at 87.4% transparency (80.0% with substrate).

To achieve the inert top-coating process, we used non-toxic and non-flammable hydrofluoroethers (HFEs) as inert solvents in our nanowire dispersion. These so-called orthogonal solvents are highly fluorinated and are used in our lab for photolithography.[14–16] They dissolve other fluorinated molecules, but do not damage non-fluorinated materials. OLED stacks with organic semiconductors stay operational even in boiling HFE.[17]

An OSC with an AgNW top-electrode is successfully prepared and shows an efficiency of 1.23% similar to that using an evaporated thin metal electrode having an efficiency of 1.10% after comparable air exposure. We have discussed the possibility of enhancing PCE by optimization of the spray-coating process.

Experimental

For easier sample handling, all the experiments were performed on cleaned 2.5 × 2.5 cm^2 BK7 glass substrates (Schott, Mainz, Germany) and pre-treated by oxygen plasma.

Silver nanowires (AgNWs) SLV-NW-90 (Blue Nano, Charlotte (NC), USA) with a mean diameter of 90 nm and a mean length of 25 μm were obtained in ethanol.

Modification using a proprietary perfluorinated methacrylate polymer (EGC-2702 by 3M Novec):

A 0.7 ml ethanol solution of AgNW was diluted with 3.5 ml of ethanol. After a short sonication process, 3 ml of EGC-2702 were added and the mixture was magnetically stirred for 10 min. The resulting solution was transferred into 6 centrifuge tubes (2 ml volume) and centrifuged for 60 s at 13 000 rpm. Finally, the AgNWs were redispersed in 7 ml of methylnonafluoro-*n*-butylether (HFE-7100 by 3M Novec). Alternatively, the precipitated AgNWs were washed by adding 1 ml HFE-7100 into every tube, centrifuged again and then redispersed in HFE-7100.

Modification with 1H,1H,2H,2H-perfluorodecanethiol (Sigma Aldrich):

A 0.7 ml ethanol solution of AgNW was diluted with 3.5 ml of ethanol and sonicated briefly. Then the thiol was added in a 1 : 10 Ag : thiol molar ratio and the mixture was stirred at room temperature overnight or for 5 h at 50 °C. The nanowires were then washed with ethanol and HFE-7100 successively and redispersed in HFE-7100.

Finally, the dispersions were diluted to 0.2 mg ml^{-1} by adding HFE-7100 and were spray-coated with a nozzle (Fisnar, Wayne (NJ), USA) onto a substrate heated up to 30 °C or 80 °C to guarantee a fast HFE-7100 or ethanol evaporation respectively. The spraying distance, moving speed and spraying pressure of the nozzle were 12 cm, 1.5 cm s^{-1} and 200 mbar, respectively.

Transmittance measurements were performed using a UV-VIS spectrometer (Shimadzu) with an integrating sphere containing the substrate. A four point probe setup (Lucas Labs) was used for measuring the sheet resistance. A desktop SEM (FEI PHENOM) or a SEM (Carl Zeiss DSM 982) was used for acquiring scanning electron microscopy images.

Organic solar cells were produced by thermal evaporation at a base pressure of 10^{-8} mbar with a single chamber system (Lesker, Hastings, UK). The following organic materials were used as purchased or purified by gradient sublimation: C60 (CreaPhys, Dresden, Germany), zinc-phthalocyanine (ZnPc) (CreaPhys, Dresden, Germany) and *N*,*N*′-((diphenyl-*N*,*N*′-bis)-9,9,-dimethyl-fluoren-2-yl)-benzidine (BF-DPB) (Synthon, Wolfen, Germany), Novaled Dopant NDP9 and tetrakis(1,3,4,6,7,8-hexahydro-2*H*-pyrimido[1,2-*a*]pyrimidinato)ditungsten (W2(hpp)4) (Novaled Ag, Dresden, Germany), Aluminum (Lesker, Hastings, UK). A naphthalene-tetracarboxylicdiimide (NTCDI) derivate MH250 was synthesized in house.

The organic p-i-n type solar cells were built as follows: Al [100 nm]/NDP9 [1 nm]/BF-DPB : NDP9 (10 wt%) [30 nm]/ZnPc [5 nm]/ZnPc : C60 (1 : 1 volume ratio) [30 nm]/C60 [30 nm]/MH250:W2(hpp)4 (7 wt%) [50 nm]. Directly on top either the AgNWs were spray-coated under ambient conditions (6 min) or the reference transparent thin metal electrode Al [1 nm]/Ag [14 nm] was thermally evaporated in UHV.

The solar cells were illuminated through a mask (4.69 mm^2) using a sunlight simulator SoCo 1200 MHG (K.H. Steuernagel Lichttechnik GmbH, Mörenfeld-Walldorf, Germany) at an intensity of 100 mW cm^{-2} (not corrected for spectral mismatch). The corresponding *j*–*V*-curve was measured using an SMU (Keithley).

Results and discussion

Nanowire system and optimization of the electrode

We used hydrofluoroether fluids (HFE) for our experiments, as the deposition of AgNWs from water or conventional organic solvents on most OEDs causes the dissolution or rapid degradation of the active organic layers. The high fluorination level of the HFEs hinders an easy phase transfer of common AgNWs with a high yield, quality, and an aspect ratio from ethanol into these solvents. This is due to the nanowire shell material, polyvinylpyrrolidone (PVP), originating from polyol synthesis and allowing stable dispersions in polar solvents only. For the transfer of hydrophilic AgNWs/PVP to the HFE phase, the nanowire shell needs to have some fluorinated moieties extending to the solution. A high fluorination of the NW shell can be realized by either replacing the shell *via* a ligand exchange or by using an additional highly fluorinated stabilizer mixing with and maintaining the original shell.[18]

Thiols are known as effective phase-transfer agents for noble metals.[19–23] For the ligand-exchange strategy, we chose a

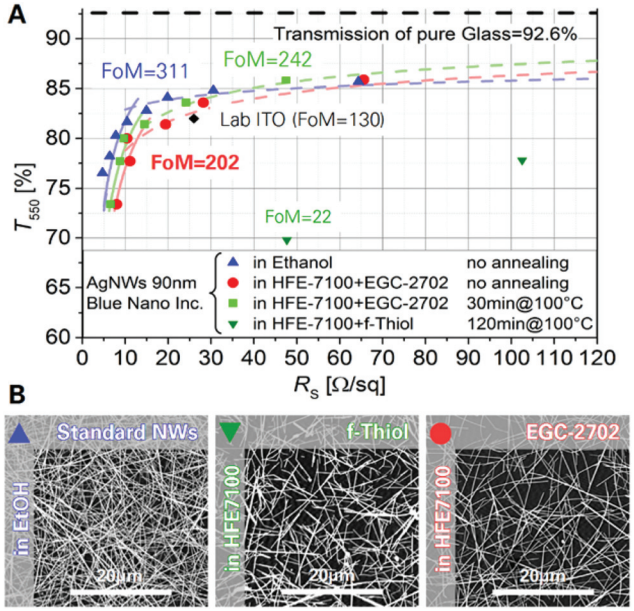

Fig. 1 (A) Integrated transmittance at 550 nm T_{550} over sheet resistance R_S of the spray-coated AgNW electrodes. Common AgNWs in ethanol (blue upright triangles), non-annealed (red circles) and annealed (light green squares) AgNWs in HFE-7100 stabilized with EGC-2702 in comparison with AgNWs in HFE-7100 stabilized with a perfluorinated thiol (dark green upside-down triangles) and our lab standard ITO (black diamond). Additionally, the values of the bulk-like figure of merit (FoM) are written next to the corresponding data and the fit curves of the FoM (solid lines) and percolative figure of merit (dashed lines) are depicted. (B) Corresponding SEM measurements of the non-annealed AgNW electrodes shown in (A).

perfluorinated thiol. For the modification of the PVP shell with the help of a stabilizer, a perfluorinated methacrylate polymer (EGC-2702, *cf.* Experimental) is used. In both cases, AgNWs are well redispersed in HFE-7100 after the modification. Due to the low boiling point of HFE-7100, the resulting dispersions could be sprayed onto the substrates at only 30 °C surface temperature, without inhomogeneous drying effects. SEM pictures of the modified AgNWs spray-coated on glass are shown in Fig. 1B. It is clearly visible that the usage of the EGC-2702 polymer keeps the wires long and flexible (*cf.* Fig. 1B right). The aspect ratio (length *vs.* diameter) of the NWs stays high, comparable with the initial wires (*cf.* Fig. 1B left). In contrast, thiol-modified NWs become shorter and stiffer (*cf.* Fig. 1B middle). Probably, this is due to the high excess of thiol needed for the phase transfer and strong bonding of the SH-group on the silver surface. Since lower aspect ratios (length *vs.* diameter) decrease the percolation in the network, consequently, the sheet resistance at equal transmittance is higher in electrodes with shorter wires. This is shown in Fig. 1A.

The opto-electrical performance of spray-coated AgNWs stabilized with EGC-2702 and dispersed in HFE-7100 is compared to common AgNWs in ethanol and to our lab standard ITO (26.0 Ω $\square^{-1}$ @ 82.0% transparency including substrate). Therefore the transmittance at 550 nm (T_{550}) over the sheet resistance is plotted, and fitted with bulk and percolation models according to De *et al.*[24] The bulk model, for the transmission and sheet resistance of planar and homogeneous films, was proposed by Glover and Tinkham.[25] This model is fairly accurate and commonly used for the comparison of such films as transparent electrodes, as it allows to compress all physical properties into a single dimensionless fitting parameter, which can be used as the figure of merit. For percolative systems like AgNWs, the model can be used for very high coverages for which the films start to behave like bulk materials. For intermediate coverages, below the bulk behaviour, but above the percolation threshold, the system can be well described by using the percolative model, as it was nicely shown by De *et al.*[24] and is depicted in Fig. 1 as well. For the data in Fig. 1, the corresponding figure of merit for the bulk model is calculated and written next to the corresponding data. The dimensionless FoM enables a direct comparison of the performance of the resulting electrodes in the low sheet resistance/high coverage range.[24]

The T_{550}–R_S data of our novel system comprising HFE-7100 and EGC-2702 effectively reproduce the typical shape of a percolation-based transparent electrode.[24] Calculating the corresponding FoM results in 202 being distinctly higher than that of ITO (FoM = 130) in the low transparency regime. The thiol-modified AgNWs yield a worse performance, exhibiting a high sheet resistance of 48.0 Ω $\square^{-1}$ at 77.4% transparency (70.0% with substrate) corresponding to an FoM of 22, probably due to a poor wire-to-wire contact or a change in the aspect ratio. As a consequence, we concentrated on the detailed investigation of the high-performance AgNW electrodes achieved with EGC-2702 as a stabilizer.

To further improve the sheet resistance of the fluorinated NW system, the influence of heating is investigated, since annealing of the NW mesh has proven beneficial for other NW systems.[1] In the case of AgNW top-electrodes deposited on OEDs, the post-annealing temperatures are limited to around 100 °C due to the low glass transition temperatures of organic materials.[26] Therefore, we apply that temperature until the sheet resistance increases again. Hereby, a slight improvement in the performance of the EGC/HFE system is achieved (*cf.* Fig. 1A), increasing the FoM/pFOM from 202/52 to 242/72. These numbers are lower compared to the more optimized PVP/AgNW bottom-electrode (non-annealed 311/36, annealed 540/145), which is deposited from ethanol. This is likely to be caused by the thicker shells of the EGC/HFE system, resulting in higher contact resistances at the wire-to-wire junctions. The effect is probably aggravated by the different drying kinetics and interaction forces from different temperatures, surface energies, and materials resulting in higher sheet resistances.

To support polymer diffusion and rearrangement on the surface during the spray process, HFEs with higher boiling points are investigated. Exchanging HFE-7100 (b.p. = 61 °C) with HFE-7200 (b.p. = 76 °C) or HFE-7300 (b.p. = 98 °C) does not lead to a significant improvement. In further experiments, the improvement of the top-electrode performance is investigated by decreasing the total amount of insulating EGC at the

interfaces between the wires and cell. Either during the preparation of the dispersion the centrifuged wires are additionally solvent-washed with HFE-7100 prior to redispersion, or the deposited electrodes are submerged in HFE-7100 to remove some ECG2702 from the nanowires. The additional washing step before redispersion was able to remove some EGC-2702 from the solution, but the deposition of the corresponding dispersion resulted in non-conductive AgNW networks ($R_S \geq 10$ kΩ $\square^{-1}$). SEM images of the washed wires (high R_S) and the non-washed wires (low R_S) are shown in the ESI(Fig. S1† bottom). In the latter case, a higher amount of the free polymer material is visible on the substrate surface which covers the wires. The XPS investigations (*cf.* Fig. S1† top) support this observation. By measuring the F1s peak (EGC-2702) and Ag3d peak (AgNWs), a higher fluorine to silver ratio was detected for the non-washed case compared to the solvent washed wires. In conclusion, a larger amount of polymer improves the sheet resistance. This observation agrees well with our recent publication.[27] In the said article, an organic matrix is deposited below the AgNWs attracting the nanowires to each other and to the substrate by capillary interactions between the shell and the sub-layer. Therefore the wires strongly bend over each other at the junctions and consequently the initial sheet resistance of the AgNW network is reduced by several orders of magnitude. Although we do not deposit a sublayer of EGC-2702, the same effect is apparently caused by the excess EGC-2702 present on the spray-coated surface. The sheet resistance of the resulting network is very low due to the interaction between the polymer, the wires and the surface during the drying process. As the polymer is obviously beneficial to the wire topography and junctions, during deposition, we still assumed that it might be possible to improve the sheet resistance by removing the insulating polymer after deposition. We tried to remove some of it after the deposition to decrease the wire-to-wire distance by submerging the sample in HFE. While a pure EGC-2702 layer can be easily removed from glass with HFE, EGC is still present on an AgNW electrode even after three days of being submerged in HFE at 80 °C. During that time or by changing the temperature and duration, as well as the type of HFE no sheet resistance reduction is measured.

Besides providing the high performance needed for a TCE, the dispersion consisting of AgNWs stabilized with EGC-2702 fulfills another crucial criterion. It is very stable, since even after 4 weeks of ambient air exposure, spray-coating of the AgNW/EGC dispersion leads to reproducible performances of the resulting electrodes.

Solar cells

After a successful optimization of the material and the coating process, we deposited the novel inert nanowire dispersion onto an organic small molecule-based solar cell. For this purpose, a simple cell architecture is used to exclude any unwanted side-effects. We used a ZnPc : C60 bulk heterojunction (BHJ) as the photoactive layer in a p-i-n type architecture. From our experience, this structure is reasonably air stable under short exposure. This is highly required for the NW top-electrode deposition as our spray-coating system operates under ambient conditions. Still, the time of air exposure is kept as short as possible. All other processing steps are performed under inert conditions, such as a glovebox or a UHV. During the spray-coating of the AgNW top-electrode, the same amount of AgNWs is simultaneously deposited on a separate glass substrate. Measuring the resulting stand-alone electrode film enables a simple non-destructive way for estimating the sheet resistance and transmittance of the corresponding top-electrode on the device. This stand-alone electrode exhibits a sheet resistance of 15.0 Ω $\square^{-1}$ at 88.4% transparency (81.0% with substrate) and an FoM of 192.

The *j*–*V*-characteristics and the characteristic parameters of the best pixels of the obtained solar cell devices are depicted in Fig. 2 and Table 1, respectively. The initial performance of the as-prepared cell is very poor. Storing for 3 h under the nitrogen atmosphere of a glovebox has no remarkable influence on the shape of the *j*–*V*-curve and the PCE of the device. The deposition of 50 nm n-doped electron transport layer (n-ETL) onto the whole solar cell enables a significant increase of the PCE to 0.76%. This improvement is based on the increased

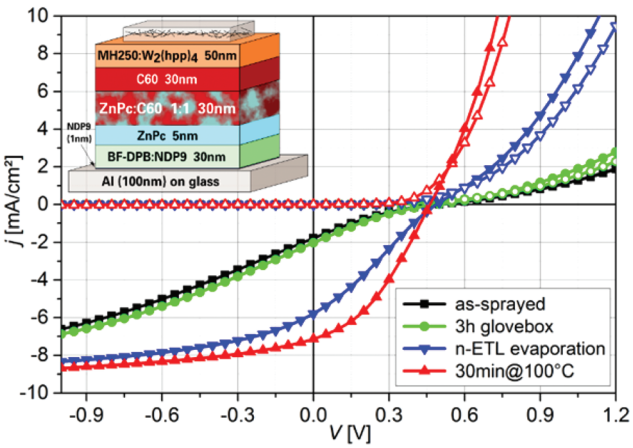

Fig. 2 Current–voltage-characteristics of a dark and illuminated organic p-i-n type solar cell with a ZnPc : C60 (1 : 1, 30 nm) bulk heterojunction as the photoactive layer. The device performance after successive treatments is plotted: Directly after spray-coating of AgNWs (black squares), after storing for 3 h in a glovebox (green circles), after evaporation of 50 nm n-ETL (blue upside-down triangles) and after annealing for 30 min at 100 °C in a glovebox (red upright triangles).

Table 1 Characteristic parameters of the solar cells in Fig. 2

Treatment	j_{SC}[a] [mA cm^{-2}]	V_{OC} [V]	FF [%]	η^b [%]	Sat	I^b [mW cm^{-2}]
As-prepared	1.78	0.50	17.6	0.16	3.73	100
N2	2.02	0.49	18.7	0.18	3.41	101
n-ETL	5.79	0.49	27.0	0.76	1.44	100
Annealing	7.14	0.46	37.2	1.23	1.22	100

[a] Measured with a mask. [b] Not corrected for spectral mismatch.

short circuit current density j_{SC} and on the increased fill factor FF. However, the shape of the curve is still s-like. This kink is strongly reduced by annealing (30 min@100 °C) within the glovebox. Thereby, a gain in the PCE by 62% to 1.23% is observed, again due to the increasing values of the j_{SC} and the FF.

A detailed discussion enables a deeper understanding of the observed *j–V*-behaviour. The open circuit voltage V_{OC} (0.50 V) of the as-prepared device is only slightly lower than the expected values for the non-annealed ZnPc : C60 (1 : 1) BHJs (0.51 V)[28] indicating the electrical integrity of the photoactive layer. In particular, the short circuit current density j_{SC} (1.78 mA cm^{-2}) and the fill factor (17.6%) are very low resulting in a poor PCE of the solar cell (0.16%). Additionally, the saturation factor Sat (3.73) is high and the current slope in the forward direction is fairly low. Most likely, the non-air-stable n-dopant W2(hpp)4 of the ETL is affected by oxygen and the electrical contact at the interface between the nanowires and the cell is poor due to the remaining EGC-2702. These effects might cause injection or extraction barriers at the interfaces between transport layers and contacts, which are known to cause s-kink like *j–V*-behavior.[29,30]

Storing of the nanowire cell for three hours up to three days in a nitrogen atmosphere to remove the remaining humidity has no significant influence on the device performance (*cf.* corresponding *j–V*-characteristics). Therefore, we deposited an additional highly n-doped ETL directly onto the complete device. The resulting layer embeds the nanowires, improves the contact with the film below and introduces a fresh, non-oxidized n-doped layer, to ensure a good ohmic contact. Therefore, we expect a strong improvement in the extraction barrier between the AgNWs and the initial n-ETL. However, the "s-kink" remains visible, whereas the device performance increases remarkably. While the V_{OC} remains constant at 0.49 V, the j_{SC} increases to 5.79 mA cm^{-2} and the FF to 27.0% resulting in a tripled PCE of 0.76%. At the same time the Sat decreases to 1.44 while the forward current strongly increases. This indicates a higher charge selectivity and an increased conductivity of the n-doped transport layer.

By applying a post-annealing step at 100 °C for 30 min, we expect the removal of the residual water and oxygen, and an interdiffusion of the materials and n-dopants at the NW–ETL interface, plus maybe a small thermal reactivation of some passivated n-dopants to improve the contact and the cell. As a result, the "s-kink" vanishes in the corresponding *j–V*-curve. Consequently, the PCE rises to 1.26%, accompanied by an increased j_{SC} (7.14 mA cm^{-2}) and a higher FF (37.2%). By applying another post-annealing step at 100 °C for 30 min, the device is completely destroyed. This is most likely the result of a messed up BHJ from the diffusion or phase segregation, as visible in the step-by-step decrease of V_{OC} (0.50–0.46 V).

Fig. 3 depicts the *j–V*-characteristics of equally fabricated cells with different top-electrodes, enabling an investigation of the influence of the inevitable air exposure of the NW device. We prepared a reference solar cell (ref cell) with a transparent top-electrode consisting of an evaporated thin metal film (1 nm Al/14 nm Ag) and a 65 nm Alq3 capping layer[31] (never

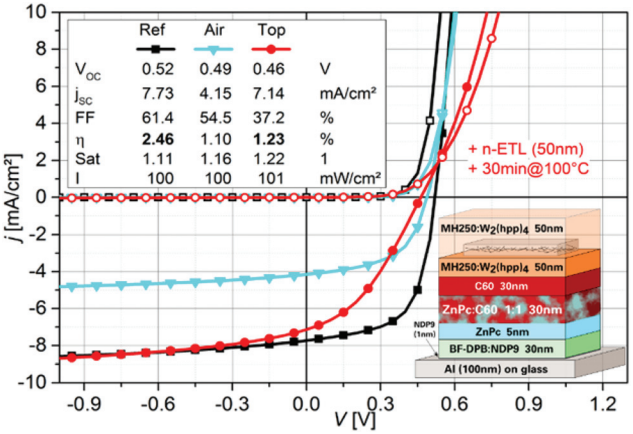

Fig. 3 Current–voltage-characteristics of dark and illuminated organic p-i-n type solar cells with a ZnPc : C60 (1 : 1, 30 nm) bulk heterojunction as the photoactive layer. The device comprising a spray-coated AgNW transparent top-electrode (red circles) is compared to a reference cell with a transparent thin metal top-electrode (Al [1 nm]/Ag [14 nm]) (black squares) and a solar cell being exposed exactly the same time to air than the top device before the thermal evaporation of the thin metal top-electrode in UHV (cyan triangles). The unfilled symbols represent the corresponding dark curves.

exposed to air) and compared it to the top-electrode NW cell from Fig. 2. During spray-coating of the top cell, a reference cell with the same device stack is exposed exactly for the same time to air (air cell) and is, subsequently, coated with a thin metal top-electrode (1 nm Al/14 nm Ag, without capping) by thermal evaporation in UHV. The NW top cell exhibits a PCE of 1.23%, higher than the air cell showing 1.10%. However, the inertly prepared ref cell shows a twice as high PCE of 2.46%, exhibiting the highest V_{OC}, j_{SC}, FF as well as the lowest Sat. The top cell's j_{SC} of 7.14 mA cm^{-2} is comparable to the value of the ref cell proving that most of the charges can be extracted under short circuit conditions. Although the "s-kink" and therefore the extraction barrier vanishes, there is still a poor charge extraction as can be seen in the lower FF of 35.1% (NW top cell) instead of 61.4% (ref cell). The electrical contact between NWs and ETL seems to be worse than between the evaporated thin metal and the ETL. Hot metal can easily diffuse inside the organic material and can establish a strong electrical connection during evaporation, whereas the AgNWs are supposed to lie on top of the organic interface being partially insulated by excess EGC and PVP stabilizers. The resulting poor contact is probably further aggravated by the partially passivated n-dopant. This argument is supported by the comparable FF of the air cell (54.5%) with the ref cell (61.4%), whereas the top cell exhibits 37.2%. Regarding the j_{SC}, we observe a lower value of 4.15 mA cm^{-2} (air cell) instead of 7.14 mA cm^{-2} (top cell). An additional capping layer will improve the j_{SC}, but will not be sufficient to reach the j_{SC} level of the top cell, pointing to some damage or passivation from the air exposure. Therefore an annealing step under the same conditions is applied to recover the air cell. As a result, the current does not increase significantly (*cf.* Fig. S2†), indicating

some damage by air exposure that needs to be accounted for in the NW cell as well.

In summary, we were able to apply our novel AgNW top-electrode on top of simple ZnPc : C60 devices. The cells show reasonable efficiencies, but lose a bit of performance due to an inevitable air exposure during spray-coating and some interface contact trouble at the NW device interface, which is not yet optimized. Thus, the successful preparation and top-deposition of an inert nanowire dispersion on top of a sensible organic device has been demonstrated, with the transparent electrode achieving a competitive performance.

Conclusions

We have developed an inert AgNW dispersion and successfully demonstrated a spray-coating process for the deposition of silver nanowires (AgNWs) onto vacuum-processed small molecule organic electronic devices for the first time. Using commonly synthesized AgNWs and a perfluorinated methacrylate to modify the nanowire shell enables dispersion in highly fluorinated solvents. These inert solvents do not dissolve the organic materials used in our solar cells and are compatible with most of the small molecules and polymers used in organic electronics in general. Spray-coating of the inert AgNW dispersion leads to high performance electrodes. They show a very good performance, exhibiting a sheet resistance of 10.0 $\Omega\ \square^{-1}$ at 87.4% transparency (80.0% with substrate) directly after a low temperature deposition at 30 °C without further post-processing. Finally, we present the successful deposition of our inert AgNW dispersion onto the vacuum-processed and solvent-sensible organic p-i-n type solar cells. The simple, air-exposed devices exhibit reasonable PCEs of 1.23%, similar to the reference device. Thus, we were able to demonstrate the first small molecule-based organic solar cell successfully employing a spray-coated AgNW transparent top-electrode.

Acknowledgements

This work was funded by the European Community's Seventh Framework Program (FP7/2007-2013) under grant agreement No. 314068 (Project TREASORES) and within the DFG Cluster of Excellence 'Center for Advancing Electronics Dresden'. We thank Susanne Goldberg from TU Dresden for the SEM measurements and Andreas Wendel and the rest of the Lesker-Team of IAPP, TU Dresden for the solar cell preparation as well as Martin Schwarze from IAPP, TU Dresden for the XPS measurements.

Notes and references

1 C. Sachse, L. Müller-Meskamp, L. Bormann, Y. H. Kim, F. Lehnert, A. Philipp, B. Beyer and K. Leo, *Org. Electron.*, 2013, **14**, 143.
2 F. Guo, X. Zhu, K. Forberich, J. Krantz, T. Stubhan, M. Salinas, M. Halik, S. Spallek, B. Butz, E. Spiecker, T. Ameri, N. Li, P. Kubis, D. M. Guldi, G. Matt and C. J. Brabec, *Adv. Energy Mater.*, 2013, **3**, 1062.
3 C. Sachse, N. Weiß, N. Gaponik, L. Müller-Meskamp, A. Eychmueller and K. Leo, *Adv. Energy Mater.*, 2014, **4**, 1300737.
4 M. Song, D. S. You, K. Lim, S. Park, S. Jung, C. S. Kim, D.-G. Kim, J.-K. Kim, J. Park, Y.-C. Kang, J. Heo, S.-H. Jin, J. H. Park and J.-W. Kang, *Adv. Funct. Mater.*, 2013, **23**, 4177.
5 C. Preston, Y. Xu, X. Han, J. N. Munday and L. Hu, *Nano Res.*, 2013, **6**, 461.
6 D. H. Wang, D. Y. Kim, K. W. Choi, J. H. Seo, S. H. Im, J. H. Park, O. O. Park and A. J. Heeger, *Angew. Chem., Int. Ed.*, 2011, **50**, 5519.
7 L. Müller-Meskamp, Y. H. Kim, T. Roch, S. Hofmann, R. Scholz, S. Eckardt, K. Leo and A. F. Lasagni, *Adv. Mater.*, 2012, **24**, 906.
8 H.-W. Chang, J. Lee, S. Hofmann, Y. H. Kim, L. Müller-Meskamp, B. Lüssem, C.-C. Wu, K. Leo and M. C. Gather, *J. Appl. Phys.*, 2013, **113**, 204502.
9 W. Gaynor, S. Hofmann, M. G. Christoforo, C. Sachse, S. Mehra, A. Salleo, M. D. McGehee, M. C. Gather, B. Lüssem, L. Müller-Meskamp, P. Peumans and K. Leo, *Adv. Mater.*, 2013, **25**, 4006.
10 J.-Y. Lee, S. T. Connor, Y. Cui and P. Peumans, *Nano Lett.*, 2010, **10**, 1276.
11 J. Krantz, T. Stubhan, M. Richter, S. Spallek, I. Litzov, G. Matt, E. Spiecker and C. J. Brabec, *Adv. Funct. Mater.*, 2013, **23**, 1711.
12 M. Reinhard, R. Eckstein, A. Slobodskyy, U. Lemmer and A. Colsmann, *Org. Electron.*, 2013, **14**, 273.
13 G. Y. Margulis, M. G. Christoforo, D. Lam, Z. M. Beiley, A. R. Bowring, C. D. Bailie, A. Salleo and M. D. McGehee, *Adv. Energy Mater.*, 2013, **3**, 1657.
14 A. A. Zakhidov, J.-K. Lee, H. H. Fong, J. A. DeFranco, M. Chatzichristidi, P. G. Taylor, C. K. Ober and G. G. Malliaras, *Adv. Mater.*, 2008, **20**, 3481.
15 J.-K. Lee, P. G. Taylor, A. A. Zakhidov, H. H. Fong, H. S. Hwang, M. Chatzichristidi, G. G. Malliaras and C. K. Ober, *J. Photopolym. Sci. Technol.*, 2009, **22**, 565.
16 S. Krotkus, F. Ventsch, D. Kasemann, A. A. Zakhidov, S. Hofmann, K. Leo and M. C. Gather, *Adv. Opt. Mater.*, 2014, **2**, 1043.
17 A. A. Zakhidov, S. Reineke, B. Lüssem and K. Leo, *Org. Electron.*, 2012, **13**, 356.
18 R. A. Sperling and W. J. Parak, *Philos. Trans. R. Soc. London, Ser. A*, 2010, **368**, 1333.
19 K. V. Sarathy, G. Raina, R. T. Yadav, G. U. Kulkarni and C. N. R. Rao, *J. Phys. Chem. B*, 1997, **101**, 9876.
20 R. Sardar, J.-W. Park and J. S. Shumaker-Parry, *Langmuir*, 2007, **23**, 11883.
21 H. Hiramatsu and F. E. Osterloh, *Chem. Mater.*, 2004, **16**, 2509.
22 T. Yonezawa, S. Onoue and N. Kimizuka, *Langmuir*, 2001, **17**, 2291.

23 P. S. Shah, J. D. Holmes, R. C. Doty, K. P. Johnston and B. A. Korgel, *J. Am. Chem. Soc.*, 2000, **122**, 4245.
24 S. De, P. J. King, P. E. Lyons, U. Khan and J. N. Coleman, *ACS Nano*, 2010, **4**, 7064.
25 R. E. Glover and M. Tinkham, *Phys. Rev.*, 1957, **108**, 243.
26 Y. Shirotaab, *J. Mater. Chem.*, 2005, **15**, 75.
27 F. Selzer, N. Weiß, L. Bormann, C. Sachse, N. Gaponik, L. Müller-Meskamp, A. Eychmüller and K. Leo, *Org. Electron.*, 2014, **15**, 3818.
28 F. Selzer, C. Falkenberg, M. Hamburger, M. Baumgarten, K. Müllen, K. Leo and M. Riede, *J. Appl. Phys.*, 2014, **115**, 054515.
29 W. Tress, S. Pfützner, K. Leo and M. Riede, *J. Photon. Energy*, 2011, **1**, 011114.
30 W. Tress, S. Corvers, K. Leo and M. Riede, *Adv. Energy Mater.*, 2013, **3**, 873.
31 S. Schubert, J. Meiss, L. Müller-Meskamp and K. Leo, *Adv. Energy Mater.*, 2013, **3**, 438.